RESEARCH ARTICLE

RUNNING HEAD: Kinematic and neuromuscular gait control under constraints

Kinematic and neuromuscular characterization of cognitive involvement in gait control in healthy young adults

Valentin Lana[1], Julien Frère[2], Vincent Cabibel[1], Tristan Réguème[1], Nicolas Lefèvre[3], Elodie Vlamynck[1], Leslie M. Decker[1,3,*]

[1] Normandie Univ, UNICAEN, INSERM, COMETE, GIP Cyceron, Caen, France.
[2] Univ. Grenoble Alpes, CNRS, Grenoble INP, GIPSA-Lab, Grenoble, France.
[3] Normandie Univ, UNICAEN, CIREVE, Caen, France.

Correspondence:
Leslie Marion DECKER
UMR-S 1075, INSERM / UNICAEN
COMETE – Mobilités : Vieillissement, Pathologie, Santé
Pôle des Formations et de Recherche en Santé
2, Rue des Rochambelles, 14032 Caen Cedex 5
Electronic address: leslie.decker@unicaen.fr
Phone: +33 (0)6 70 40 58 44

ABSTRACT

The signature of cognitive involvement in gait control has rarely been studied using both kinematic and neuromuscular features. The present study aimed to address this gap. Twenty-four healthy young adults walked on an instrumented treadmill in a virtual environment under two optic flow conditions: normal (NOF) and perturbed (POF, continuous mediolateral pseudo-random oscillations). Each condition was performed under single-task and dual-task conditions of increasing difficulty (1-, 2-, 3-back). Subjective mental workload (raw NASA-TLX), cognitive performance (mean reaction time and d-prime), kinematic (steadiness, variability and complexity in the mediolateral and anteroposterior directions) and neuromuscular (duration and variability of motor primitives) control of gait were assessed. The cognitive performance and the number and composition of motor modules were unaffected by simultaneous walking, regardless of the optic flow condition. Kinematic and neuromuscular variability was greater under POF compared to NOF conditions. Young adults sought to counteract POF by rapidly correcting task-relevant gait fluctuations. The depletion of cognitive resources through dual-tasking led to reduced kinematic and neuromuscular variability but this occurred to the same extent regardless of simultaneous WM load. Increasing WM load led to a prioritization of gait control in the ML direction over the AP direction. The impact of POF on kinematic variability (step velocity) was reduced when a cognitive task was performed simultaneously, but this phenomenon was no more pronounced with increasing WM load. Collectively, these findings highlight the kinematic and neuromuscular adjustments in gait control associated with the separate and joint effects of cognitive and visual constraints during treadmill walking.

NEW & NOTEWORTHY

The kinematic and neuromuscular signatures of cognitive involvement in gait control have rarely been studied jointly. We sought to address this issue using gait perturbation and dual-task paradigms. The protocol consisted of a fixed-speed treadmill walk to which visual and cognitive constraints were applied separately and together. The results revealed that young adults optimally regulated their gait to cope with these constraints by maintaining relatively stable muscle synergies and flexibly allocating attentional resources.

Gait; muscle synergies; motor variability; nonlinear dynamics; executive control.

INTRODUCTION

Walking is usually considered to be a simple and automatic behavior relying on the central pattern generators, present in the spinal cord (1, 2). However, walking in complex environments of everyday life requires the brain to continuously adapt to external sensory inputs such as obstacles or irregular surfaces (3) and to internal cognitively demanding tasks (4). To this end, the central nervous system controls locomotion in a hierarchical and distributed manner by modulating the activity of its control subsystems such as CPG (5, 6). Then, these networks are modulated by descending cortical and brainstem pathways as well as by sensory feedback to regulate the movement in progress (7, 8). These mechanisms allow the control of the multiple joints and muscle groups in order to cope with the associated large degrees of freedom (9).

At neuromuscular level, to simplify the development of complex movements, it has been proposed that the central nervous system (CNS) relies on a limited number of low-dimensional structures called muscle synergies (10, 11). In this sense, the changes observed refer to the flexibility of the modular organization. Each synergy contains a spatial component (or a motor module) that represents the involvement of each muscle within the synergy and a temporal component (or a motor primitive) that reflects its activation profile (12). On the one hand, the number and composition of motor modules is invariable under sensory perturbations in healthy adults (*e.g.* optic flow, 13). On the other hand, Santuz et al. (14) observed an increase in the duration of motor primitives when walking was perturbed by continuous lateral oscillations of the support surface (*i.e.* mechanical perturbations). This increase was interpreted as a compensatory mechanism implemented by the CNS (*i.e.* high cognitive cost) under increased postural threat (15). To our knowledge, no study has assessed the

extent to which the modification of gait control under visual perturbations requires attentional resources (*i.e.* cognitive cost) and modulates the underlying muscle synergies. Only Walsh (16) assessed the modulation of muscle synergies during walking and running by performing a concurrent cognitive task (counting backwards from 7 to 7). However, he did not observe any significant effects of the dual task on the duration of motor primitives.

Under dual-task conditions, the cognitive involvement associated with regulation of gait relies on many factors, including the type and complexity of the two tasks (17). Executive functions (*i.e.* "higher-level" cognitive functions) in particular "divided attention" (18) and "working memory" (19) are involved to control and regulate "lower-level" cognitive processes and goal-directed actions (20, 21). In this way, these functions are needed to regulate the variables relevant to satisfy the locomotor task goal such as step velocity on a fixed speed treadmill (22, 23). This result remains to be confirmed in other contexts. Depending on the constraints associated with the environment and the task, it may be necessary to regulate one or more locomotor variables. Recently, Dingwell and Cusumano (24) have shown that, in the context of treadmill walking, in addition to step velocity (V), step width (W) and, to a lesser extent, lateral body position (z_B, which corresponds to the distance between the center of the treadmill and the midpoint between the two feet), are tightly regulated to maintain medio-lateral stability during walking. Also, it has been experimentally confirmed that walking under continuous lateral mechanical or visual perturbation, W and z_B were more variable but also more tightly regulated (25–27). Nevertheless, the hypothesis that executive functions are responsible for these regulation mechanisms in perturbed walking contexts has never been tested.

In fact, only two studies have evaluated the interaction effect of visual (*i.e.* optic flow) perturbations on gait under dual-task conditions (4, 28). The results of these both studies suggest that in those conditions, the participants' attentional resources would be redirected towards the performance of the concomitant cognitive task at the expense of the visual environment (29). In turn, this phenomenon could decrease the influence of ML optic flow perturbations on gait control. However, these two studies suffer from several methodological limitations, including the use of (i) non-executive cognitive tasks (*i.e.* reaction time task and Go/no go respectively) and (ii) less ecological optic flow perturbations (*i.e.* more simplistic and less realistic) than those generally used (26, 30). Thus, the involvement of cognition in optic flow processing during gait control remains to be defined.

The present study aimed to characterize cognitive involvement in gait control at the kinematic and neuromuscular levels in healthy young adults. We hypothesized that (i) Optic flow perturbations would lead to greater kinematic (*i.e.* step parameters) and neuromuscular (*i.e.* motor primitives) variability and tighter control of task-relevant gait fluctuations, (ii) Depletion of cognitive resources through dual-tasking would lead to the opposite effects, and (iii) the impact of optic flow perturbations on gait would be reduced when performing a cognitive task simultaneously, and this phenomenon would be more pronounced with increasing working memory (WM) load.

MATERIALS AND METHODS

Participants

Twenty-four healthy young adults (21.67 ± 2.28 years; 12 men and 12 women) took part in this study. Prior to the experiment, participants were interviewed regarding their health history. Exclusion criteria were: uncorrected visual impairment, any lower limb injury within the last six months, pain, functional limitations or any discomfort that may affect walking, history of vestibular, neurological or musculoskeletal disorders, body mass index of 30 or higher, sedentary lifestyle, and any medication altering the cognitive or physical abilities. The physical activity level was assessed by an adapted version of the question 1 of the Modifiable Activity Questionnaire (31). The lower limb laterality was determined by the leg used to kick a ball (32). All participants gave their written informed consent prior to the experiment. The study was approved by an Ethics Committee (IRB00012476-2020-30-11-76) and conducted with respect to the principles of the Declaration of Helsinki regarding human experimentation.

Experimental procedures

The experiment was conducted in the immersive room (dimensions: 4.80 × 9.60 × 3 m) of the Interdisciplinary Centre for Virtual Reality (CIREVE) at the University of Caen Normandie. The training session started with a familiarization of the participants to the 2 × 0.5 m walking treadmill (M-Gait, Motekforce Link, The Netherlands) followed by the determination of their preferred walking speed (PWS) according to the method of (33). Briefly, each participant started at a relatively low speed (*e.g.* 0.6 $m.s^{-1}$) which was progressively increased by 0.05 $m.s^{-1}$ increments until the participant reported being at his/her PWS. Then, walking speed was further increased by approximately 0.42 $m.s^{-1}$ and decreased in 0.05 $m.s^{-1}$ decrements until the participant reported once again being at his/her PWS.

The procedure was repeated until the ascending and descending speeds reported by the participant were close (difference below 0.1 $m.s^{-1}$). Afterwards, the participants were familiarized with the auditory N-back task with three levels of WM load (*i.e.* 1-back, 2-back, and 3-back). Each familiarization trial lasted at least 1 minute.

The testing session was composed of three blocks performed in a randomized order: (1) three N-back conditions in a seated position (*i.e.* single-task cognitive performance, STC), (2) walking under normal optic flow (NOF) conditions, and (3) walking under perturbed (oscillating) optic flow conditions (POF) in the ML direction. In the latter two blocks, the walking tasks were performed under both single-task (STW) and dual-task (DTW) conditions (*i.e.* responding to the N-back tasks). Participants were asked to walk naturally while looking straight ahead. The treadmill speed was adjusted to their PWS. The blocks (2) and (3) began and ended with a STW condition while the three DTW conditions were performed in a randomized order between the two STW conditions (34). Under dual-task conditions, no task priority instructions were given (34). Each condition lasted 3 minutes. Hence, a total of thirteen experimental conditions were performed (Figure 1).

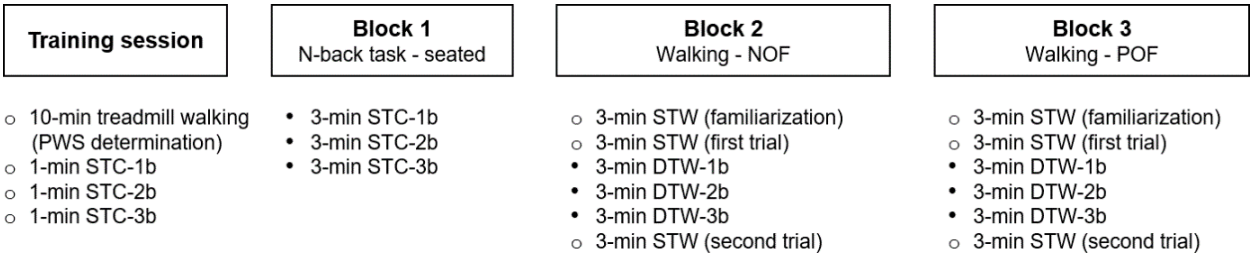

Figure 1. Experimental procedures. A training session was first performed, consisting of: 1) a 10-minute familiarization period with treadmill walking, 2) the determination of the participant's preferred walking speed (PWS) on the treadmill using the method of Jordan et al. (2007), and 3) a 1-minute familiarization trial with each of the three auditory N-back tasks, *i.e.* 1-back (1b), 2-back (2b), and 3-back (3b). Next, three experimental blocks were performed in a randomized order: 1) N-back tasks in a seated position (STC: single-task cognitive performance), 2) walking under normal optic flow (NOF), 3) walking under perturbed optic flow (POF, continuous mediolateral pseudo-random oscillations). In the last two blocks, participants began and ended with a single-task walking (STW) condition (*i.e.* free walking), while the three dual-task walking (DTW) conditions were performed in a randomized order between the two STW conditions. The experimental conditions lasted 3 minutes. Empty circles correspond to familiarization trials while solid circles correspond to experimental conditions.

At the end of each condition, participants were asked to complete the NASA task load index (NASA-TLX), a subjective multidimensional assessment questionnaire of perceived workload, on a digital tablet (35, 36). In this questionnaire, three subscales relate to the demands imposed on the

participant (*i.e.* physical, mental and temporal demands), and three others to the interaction of the participant with the task (*i.e.* effort, frustration, performance).

Manipulation of optic flow

Participants were asked to walk in a virtual environment composed of a street in ancient Rome in which white statues of 2.4 m height were spaced every 3 meters to increase motion parallax (37, 38, Figure 2). In all conditions, the velocity of the OF in the AP direction was congruent with the treadmill belt velocity. During the perturbed OF conditions, the visual field oscillated in the ML direction. The perturbation consisted of a pseudo-random sum of four sinusoids with an amplitude of 0.25 m that has previously been used in the literature (26, 30):

$$D(t) = 0.25.[1.0\sin(0.16.2\tau t) + 0.8\sin(0.21.2\tau t) + 1.4\sin(0.24.2\tau t) + 0.5\sin(0.49.2\tau t)]$$

where D(t) is the lateral translation distance (m).

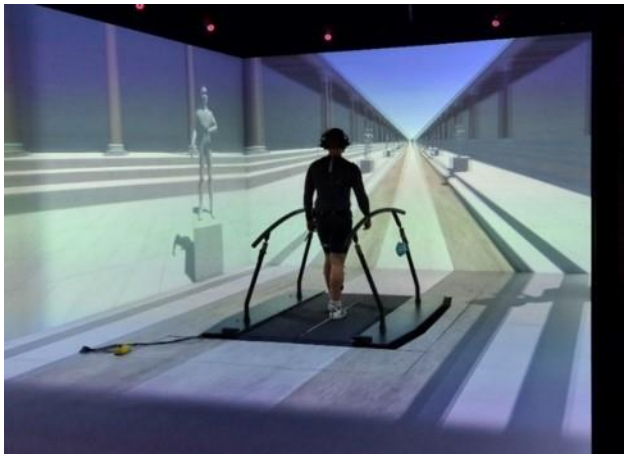

Figure 2. Experimental setup. Photograph of a participant walking on the M-Gait dual-belt instrumented treadmill (Motekforce Link, Amsterdam, The Netherlands) in a virtual environment that was developed specifically for the study. The participant wears a suit with 27 retroreflective markers (4-mm diameter) placed on specific anatomical landmarks according to an adaptation of the Plug-in-Gait full-body model (Vicon Motion Systems Ltd., Oxford, UK).

Manipulation of working memory load

N-back task was used. This task consists of a continuous sequence of auditory stimuli, presented one-by-one, in which the participant must determine if the currently presented stimulus is the same as the stimulus presented N trials before. Thus, the factor 'N' (number of items stored in WM) allows increasing the task difficulty and thus the WM load (39). Also, it involves both working memory and information processing, which has a greater impact on gait than tasks involving inhibition or visuospatial cognition, especially during perturbed walking (40). In this study, the WM load was

parametrically manipulated through three levels of an auditory N-back task. The auditory modality was chosen to avoid interfering with optic flow perturbations.

Using noise-cancelling headphones, participants easily and distinctly heard the letters "E - A - I - O - R - T" pronounced in French and were asked to answer "Yes" when the letter heard was the same as the one presented N trials earlier (*i.e.* 1-back, 2-back, 3-back). Responses were recorded using a microphone. The letters were presented with an inter-stimulus interval of 1800 to 2200 ms (2000 ± 10%) to prevent the influence of rhythm on walking (34), and a stimulus presentation duration of 500 ms. Each sequence consisted of one third of targets (*i.e.* 90 stimuli for which the participant had to answer "Yes"; 41) as well as 9 (10%), 13 (14.4%) and 16 (17.8%) lures for the 1-back, 2-back and 3-back, respectively (42). Each condition lasted 3 minutes.

Kinematic recording

The participants were equipped with 4-mm diameter retroreflective markers, fixed to specific anatomical landmarks on the body, on top of fitted clothing (43). The model used for marker placement was an adaption of the Plug-in Gait full-body model (44): only the head, trunk and lower limb markers were used for a total of 27 markers. The three-dimensional (3D) marker positions were collected at 200 Hz using 12 infrared cameras (Vero 2.2, Vicon Motion Systems Ltd., Oxford, United Kingdom). The origin of the reference frame was at the treadmill's center. Any gap in the raw motion capture data were filled using Vicon Nexus software, (version 2.8.1, Oxford Metrics, Oxford, United Kingdom). The 3D marker trajectories were then imported into MATLAB® R2020a (The MathWorks Inc., Natick, Massachusetts, USA) for further analyses.

Electromyographic recording

Once the skin prepared (*i.e.* shaving, light abrasion, cleaning with alcohol solution), surface electromyographic electrodes (EMG Trigno Snap Lead Sensors, Delsys, Inc., Natick, Massachusetts, USA) were placed on the muscles: tibialis anterior (TA), soleus (SOL), medial gastrocnemius (GAS), vastus medialis (VM), rectus femoris (RF), semitendinosus (ST), biceps femoris (BF), gluteus medius (Gmed) of the dominant lower limb (conversion A/D, 1000 Hz, 10 V). Electrodes were placed longitudinally with respect to the arrangement of muscle fibers (45) and located according to the recommendations from Surface EMG for Non-Invasive Assessment of Muscles (SENIAM; Hermens et al., 2000).

Data analysis

Subjective mental workload

In all conditions, subjective mental workload was estimated based on the Raw NASA task load index (Raw NASA-TLX, with a maximum possible score of 100 points), that is the sum of the scores of the six subscales (47).

Cognitive task performance

Mean reaction time for target trials (RT, second) and d-prime (d', a.u.) were used to assess performance on N-back tasks (48–50). The d' is the difference between the Z-score obtained from hit rate, Z_{Hit}, and that obtained from false alarms (FA, *i.e.* participant answers "Yes" when there was no target) rate, Z_{FA} (d' = Z_{Hit} - Z_{FA}; 51). The higher the hit rate and the lower the FA, the better the participant's ability to discriminate target and non-target letters. In the present experiment, a d' of 4.5 indicates 100% correct responses and no false alarms.

Gait kinematics

The kinematic data was low-pass filtered using a fourth-order zero-phase Butterworth filter with a cut-off frequency of 6 Hz. Heel strikes were computed from the heel marker trajectory using the algorithm of Zeni et al. (52). Then, step velocity (V), step width (W) and lateral body position (z_B) were extracted, as previously done (24, 26). The mean (steadiness), standard deviation (variability) and statistical persistence/anti-persistence of the time series (complexity) of these variables were then computed. To quantify how stepping fluctuations were regulated from one step to another, the detrended fluctuations analysis (DFA) scaling exponent (α), which assesses the presence and strength of statistical persistence or anti-persistence in the investigated time series, was used (22, 53–55). An α < 0.5 suggests that the time series contains anti-persistent correlations, *i.e.* subsequent deviations are more likely to be in the opposite direction, consistent with a tightly controlled process. An α = 0.5 indicates uncorrelated deviations that are attributed to noise. An α ≈ 0.5 is typically exhibited by variables that are more tightly regulated. An α >> 0.5 (*i.e.* strong persistence) is typically exhibited by variables that are less tightly regulated (22, 24, 26). Given the length of our time series (290 steps), the scaling exponent (α) was computed following the recommendations of Phinyomark et al. (56). Also, we performed a direct control analysis of step-to-step corrections to complete the DFA (57). For $q \in \{V, W, z_B\}$, participants trying to maintain a constant average value, $\bar{q}$, on the treadmill exhibit deviations away from $\bar{q}$ on any given step, $q'_n = q_n - \bar{q}$. Each such deviation is corrected on the subsequent step with a corresponding change in the opposite direction, $\Delta q_{n+1} = q_{n+1} - q_n$. From

plots of $\Delta q_{n+1} vs\ q'_n$, we computed (using least-squares regression) linear slopes and strength of correlation (R^2). Variables tightly controlled would be corrected quickly, yielding a slope value (M) close to -1 and a high R^2 value (24, 26). These variables, in particular those derived from the DFA, have demonstrated their ability to detect the involvement of cognitive control processes in gait regulation: the more tightly these variables are regulated, the greater the involvement of cognitive control (22, 23, 58).

Gait electromyography

The raw EMG signals were band-pass filtered using a fourth-order zero-phase IIR Butterworth filter with cut-off frequencies of 50 and 450 Hz, then rectified and smoothed using a fourth-order low-pass zero-phase IIR Butterworth filter with a cut-off frequency of 10 Hz (15). After subtracting the minimum, the muscle activation profiles were normalized in amplitude to the average peak activation of the selected gait cycles (*i.e.* n= 80). Lastly, each gait cycle was time-normalized to 200 points by a spline interpolation. We excluded data of 9 participants from EMG analyses because of the poor quality of the signal (*i.e.* movement-related artefacts). Therefore, EMG data from 15 right-handed participants were retained (21,67 ± 2,53 years old; BMI: 21,44 ± 1,90 kg.m^2 ; 8 men and 7 women).

For each subject and each condition, previously processed EMGs were combined into a $m \times t$ matrix where m indicates the number of muscles and t their duration of activation (original EMG matrix, EMGo). Next, muscle synergy extraction was performed by non-negative matrix factorization (NNMF; 59) of the $m \times t$ matrix corresponding to all gait cycles. The number of synergies n is specified a priori and the NNMF algorithm finds the properties of the synergies by filling two matrices: a matrix W of dimensions $m \times n$, which specifies the relative weighting of a muscle in each motor module, and a matrix C of dimensions $n \times t$, which specifies the activation over time of each motor primitive for all gait cycles. The reconstructed EMG (EMGr) of a muscle is the sum of the contributions of all the muscle synergies (60). To determine the minimum number of synergies required to correctly reconstruct EMGo, we quantified the Variance Accounted For (VAF; 61) as the ratio between the sum of the squared error values and the sum of the squared EMGo values $[VAF = \left(1 - \frac{(EMGo - EMGr)^2}{EMGo^2}\right) x\ 100]$. The number of synergies used corresponds to the one where the VAF is greater than 90% with an increment of less than 5% for s+1 synergies (61). This approach is conservative and ensures high agreement between the original and reconstructed EMG signals (60).

In each condition, motor primitives' inter-cycle variability (62, 63) and duration (15, 64) were assessed using the variance ratio (VR) and the full width at half maximum (FWHM), respectively. The latter parameter determines the number of points (percentage of cycle) exceeding half of the maximum activation of each gait cycle. Then, the values obtained from all gait cycles were averaged to obtain a single FWHM value for each condition (14).

Statistical analysis

Linear mixed models (including a random intercept for each participant) were used to compare the effect of *WM load* (1-back, 2-back, 3-back) and *Cognitive condition* (STC, DTC-NOF, DTC-POF) on cognitive performance (*i.e.* d' and RT) and subjective mental workload (*i.e.* raw NASA-TLX score) dependent variables. Where main effects were significant, relevant pairwise comparisons were conducted using marginal means estimated with Tukey's adjustment.

The performance achieved during the second STW conditions (*i.e.* performed at the end of the walking blocks) were not considered in the analysis after observing and statistically confirming a disengagement or relaxation of the participants during these conditions (Fig. S1, *Supplementary materials*). Linear mixed models (including a random intercept for each participant) were used to compare the effect of *Optic flow* (NOF, POF) and *Walking condition* (STW, DTW-1b, DTW-2b, DTW-3b) on all kinematic dependent variables (*i.e.* mean, standard deviation, α exponent, slope and R^2 for V, W, z_B). Where main effects were significant, relevant pairwise comparisons were conducted using marginal means estimated with Tukey's adjustment.

Beforehand, a chi^2 test was performed to assess the effect of *Optic flow* (NOF, POF) on the number of motor modules. A dot product (r) was used to evaluate the effect of *Walking condition* (STW, DTW-1b, DTW-2b, DTW-3b) on motor module composition. A threshold of r = 0.80 was defined below which motor modules would not be considered similar. Linear mixed models similar to those used for neuromuscular data were used to assess the effects of *Optic flow* (NOF, POF) and *Walking condition* (STW, DTW-1b, DTW-2b, DTW-3b) on motor primitives.

Linear mixed-models were fitted using the lme4 package (65) and tested on the basis of likelihood ratio tests (LRT) using the lmerTest package (66). For all variables, given that residuals are often not normally distributed (26), which was verified in our samples, parameters of model were estimated using the pbkrtest package by computing 5000 parametric bootstraps (67). Post-hoc comparison tests were performed using the emmeans package (v1.7.5). The significance threshold was set at 0.05.

Effect sizes were also examined and reported for post-hoc comparison tests using Cohen's d (d < 0.2, 0.5 < d < 0.8 and d > 0.8, indicating weak, moderate and large effects, respectively). All statistical analyses were conducted using R 4.0.5 (68).

RESULTS

Cognitive performance and subjective mental workload

A significant main effect of *WM load* was found for d' and RT (Table 1). Post-hoc tests revealed a decrease of d' (Figure 3A) and an increase of RT (Figure 3B) with increasing load. Precisely, for both dependent variables, 3-back performance was lower than 1-back and 2-back performances, and 2-back performance was also lower than 1-back performance. Significant main effects of *WM load* and *Cognitive condition* were found for the raw NASA-TLX score. Post-hoc tests revealed an increase in subjective mental workload i) with increasing load, and ii) in DTC-POF condition compared to STC and DTC-NOF conditions. No interaction effect *Cognitive condition* x *WM load* was observed (Figure 3C, Table 1).

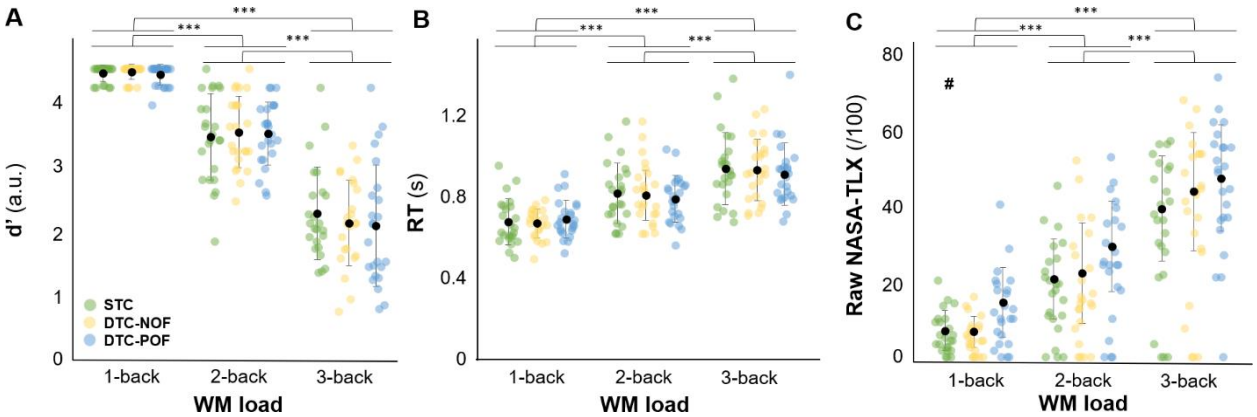

Figure 3. Cognitive performance: **A)** d-prime (d', a.u.), **B)** mean reaction time for target trials (RT, second), and **C)** raw NASA task load index (Raw NASA-TLX, the maximum score is 100), for the three N-back tasks, *i.e.* 1-back, 2-back, 3-back, performed under three cognitive conditions, *i.e.* single-task cognitive performance in a seated position (STC, green circles), dual-task cognitive performance while walking with normal optic flow (DTC-NOF, yellow circles) and perturbed optic flow (DTC-POF, blue circles). Black dots represent the mean and the error bars correspond to standard deviations. *: significant differences between the three task loads (* p < .05, ** p < .01, *** p < .001). #: significant differences between DTC-POF and the other conditions (STC and DTC-NOF).

Table 1. Statistical results for cognitive dependent variables: cognitive task performance, *i.e.* mean reaction time for target trials (RT, second) and d-prime (d', a.u.), and subjective mental workload, *i.e.* raw NASA-TLX score.

Variables		Main effect *cognitive condition*	Main effect *WM load*	Interaction effect *cognitive condition x WM load*	Estimated marginal means *post-hoc tests (Tukey's correction)*
N-back tasks	*d' (a.u.)*	LRT = 0.491 p = 0.774	**LRT = 334.4** **p < 0.001**	LRT = 2.133 p = 0.724	**WM load** 1b - 2b: t_{184} = 12.14, p < 0.001, d = 2.020 1b - 3b: t_{184} = 29.47, p < 0.001, d = 4.910 2b - 3b: t_{184} = 17.33, p < 0.001, d = 2.890
	Mean reaction time (s)	LRT = 0.987 p = 0.624	**LRT = 187.6** **p < 0.001**	LRT = 2.715 p = 0.621	**WM load** 1b - 2b: t_{184} = -8.889, p < 0.001, d = -1.480 1b - 3b: t_{184} = -17.63, p < 0.001, d = -2.940 2b - 3b: t_{184} = -8.743, p < 0.001, d = -1.460
Raw NASA-TLX	*Score (%)*	**LRT = 25.58** **p < 0.001**	**LRT = 229.6** **p < 0.001**	LRT = 1.499 p = 0.831	**Cognitive condition** NOF - POF: t_{184} = -3.767, p < 0.001, d = -0.628 POF - ST: t_{184} = 4.863, p < 0.001, d = 0.811 **WM load** 1b - 2b: t_{184} = -10.37, p < 0.001, d = -1.730 1b - 3b: t_{184} = -22.07, p < 0.001, d = -3.680 2b - 3b: t_{184} = -11.69, p < 0.001, d = -1.950

Gait kinematics

Gait steadiness (mean)

A significant main effect of *Optic flow* was found for mean W and mean z_B (Table 2). Post-hoc tests revealed an increase in mean W and a decrease in mean z_B in POF compared to NOF conditions. No interaction effect *Optic flow* x *Walking condition* was observed (Figure S2A).

Table 2. Statistical results for gait dependent variables: kinematics, *i.e.* steadiness (mean), variability (SD: standard deviation) and complexity (α: alpha exponent, M: least-squares regression linear slope, R^2: strength of correlation) of step width (W), lateral body position (z_B) and step velocity (V), and electromyography, *i.e.* motor primitive variability (VR: variance ratio) and motor primitive duration (FWHM: full width at half maximum).

Variables		Main effect *optic flow*	Main effect *walking condition*	Interaction effect *optic flow x walking condition*	Estimated marginal means *post-hoc tests (Tukey's correction)*
Mean	*W (m)*	**LRT = 54.61** **p < 0.001**	LRT = 3.285 p = 0.363	LRT = 5.997 p = 0.123	**Optic flow** NOF - POF: t_{133} = -8.138, p < 0.001, d = -1.290
	z_B (m)	**LRT = 4.573** **p = 0.036**	LRT = 2.299 p = 0.526	LRT = 1.766 p = 0.640	**Optic flow** NOF - POF: t_{133} = 2.115, p = 0.040, d = 0.334
Standard deviation (SD)	*W (m)*	**LRT = 139.7** **p < 0.001**	LRT = 2.495 p = 0.488	LRT = 2.686 p = 0.465	**Optic flow** NOF - POF: t_{133} = -15.24, p < 0.001, d = -2.410
	z_B (m)	**LRT = 122.9** **p < 0.001**	LRT = 3.294 p = 0.358	LRT = 2.608 p = 0.469	**Optic flow** NOF - POF: t_{133} = -13.80, p < 0.001, d = -2.180
	V ($m.s^{-1}$)	**LRT = 38.53** **p < 0.001**	**LRT = 13.45** **p = 0.005**	**LRT = 10.99** **p = 0.016**	**Interaction** STW NOF - STW POF: t_{133} = -5.941, p < 0.001, d = -1.878 DTW-1b POF - STW POF: t_{133} = -4.050, p = 0.022, d = -1.281 DTW-2b POF - STW POF: t_{133} = -3.780, p = 0.006, d = -1.196

					DTW-3b POF - STW POF: t_{133} = -4.861, p < 0.001, d = -1.537
DFA scaling exponent (α)	*W (a.u.)*	LRT = 1.267 p = 0.257	**LRT = 10.18** **p = 0.015**	LRT = 0.909 p = 0.834	**Walking condition** DTW-2b - STW: t_{133} = -3.047, p = 0.015, d = -0.681
	z_B (a.u.)	**LRT = 119.1** **p < 0.001**	LRT = 2.036 p = 0.582	LRT = 1.487 p = 0.694	**Optic flow** NOF - POF: t_{133} = 13.37, p < 0.001, d = 2.110
	V (a.u.)	**LRT = 5.998** **p = 0.017**	**LRT = 9.109** **p = 0.033**	LRT = 1.550 p = 0.679	**Optic flow** NOF - POF: t_{133} = 2.426, p < 0.001, d = 0.384 **Walking condition** DTW-1b - DTW-3b: t_{133} = -3.004, p = 0.016, d = -0.672
Least-squares regression linear slopes (M)	*W (a.u.)*	**LRT = 49.82** **p < 0.001**	LRT = 0.619 p = 0.887	LRT = 0.135 p = 0.987	**Optic flow** NOF - POF: t_{133} = 7.544, p < 0.001, d = 1.190
	z_B (a.u.)	**LRT = 57.65** **p < 0.001**	LRT = 0.722 p = 0.874	LRT = 6.519 p = 0.109	**Optic flow** NOF - POF: t_{133} = 8.426, p < 0.001, d = 1.330
	V (a.u.)	LRT = 2.040 p = 0.157	LRT = 2.524 p = 0.478	LRT = 0.859 p 0.836	
Strength of correlation (R^2)	*W (a.u.)*	**LRT = 49.46** **p < 0.001**	LRT = 0.609 p = 0.895	LRT = 0.151 p = 0.988	**Optic flow** NOF - POF: t_{133} = -7.421, p < 0.001, d = -1.170
	z_B (a.u.)	**LRT = 57.69** **p < 0.001**	LRT = 0.390 p = 0.941	LRT = 6.357 p = 0.106	**Optic flow** NOF - POF: t_{133} = -8.424, p < 0.001, d = -1.330
	V (a.u.)	LRT = 2.206 p = 0.144	LRT = 2.401 p = 0.508	LRT = 0.675 p = 0.898	
Variance ratio (VR)	*Primitive 1 (a.u.)*	**LRT = 4.457** **p = 0.037**	LRT = 3.265 p = 0.368	LRT = 1.519 p = 0.699	**Optic flow** NOF - POF : t_{98} = -2.109, p = 0.037, d = -0.385
	Primitive 2 (a.u.)	**LRT = 21.08** **p < 0.001**	**LRT = 20.71** **p < 0.001**	LRT = 4.569 p = 0.230	**Optic flow** NOF - POF: t_{98} = -5.265, p < 0.001, d = -0.961 **Walking condition** DTW-1b - STW: t_{98} = -3.369, p = 0.006, d = -0.867 DTW-2b - STW: t_{98} = -4.232, p < 0.001, d = -1.117 DTW-3b - STW: t_{98} = -3.623, p = 0.003, d = -0.935
	Primitive 3 (a.u.)	LRT = 0.068 p = 0.796	LRT = 4.196 p = 0.257	LRT = 0.419 p = 0.939	
	Primitive 4 (a.u.)	**LRT = 12.29** **p = 0.001**	LRT = 5.078 p = 0.177	LRT = 2.066 p = 0.588	**Optic flow** NOF - POF : t_{98} = -3.610, p < 0.001, d = -0.659
Full width at half maximum (FWHM)	*Primitive 1 (%)*	LRT = 0.822 p = 0.373	LRT = 1.568 p = 0.682	LRT = 3.834 p = 0.309	
	Primitive 2 (%)	LRT = 1.864 p = 0.177	**LRT = 10.66** **p = 0.013**	LRT = 1.027 p = 0.815	**Walking condition** DTW-1b - STW : t_{98} = 2.857, p = 0.026, d = 0.738
	Primitive 3 (%)	LRT = 3.227 p = 0.075	LRT = 0.432 p = 0.936	LRT = 0.745 p = 0.881	
	Primitive 4 (%)	LRT = 0.197 p = 0.650	LRT = 0.803 p = 0.852	LRT = 2.314 p = 0.542	

Gait variability (SD: standard deviation)

A significant main effect of *Optic flow* was found for standard deviation (SD) of W, z_B and V (Table 2, Figure S2A). Post-hoc tests revealed increased SD values in POF compared to NOF conditions (Figure 5A). A significant interaction effect *Optic flow* x *Walking condition* was found for SD of V, revealing that the effect of *Walking condition* occurred only under POF. Post-hoc tests revealed a reduction in SD of V in all DTW-POF conditions compared to the STW-POF condition, but this dual-task-related reduction was not influenced (modulated) by the level of concomitant WM load (Figure 4).

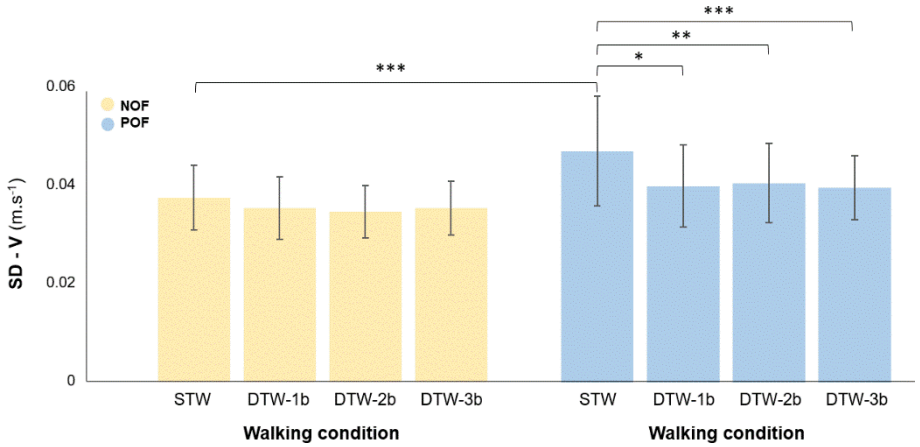

Figure 4. Interaction effect *Optic flow* x *Walking condition* for variability (SD: standard deviation) of step velocity (V). The four walking conditions: single-task walking (STW) and dual-task walking (DTW), *i.e.* walking while simultaneously responding to auditory 1-back (DTW-1b), 2-back (DTW-2b), and 3-back (DTW-3b) tasks, performed under two optic flow conditions, *i.e.* normal optic flow (NOF, yellow bars) and perturbed optic flow (POF, blue bars) are represented. *: significant differences between the four conditions (* $p < .05$, ** $p < .01$, *** $p < .001$).

Gait complexity (α: alpha exponent, M: least-squares regression linear slope, R^2: strength of correlation)

A significant main effect of *Optic flow* was found for scaling exponent (α) of z_B, α of V, slope (M) of W and M of z_B (Table 2, Figure S2). Post-hoc tests revealed an increase in anti-persistence of V and a decrease in persistence of z_B in POF compared to NOF conditions (Figure 5B). Furthermore, they revealed a more negative slope value (closer to -1) and a higher R^2 value for W and z_B in POF compared to NOF conditions (Figure 5C).

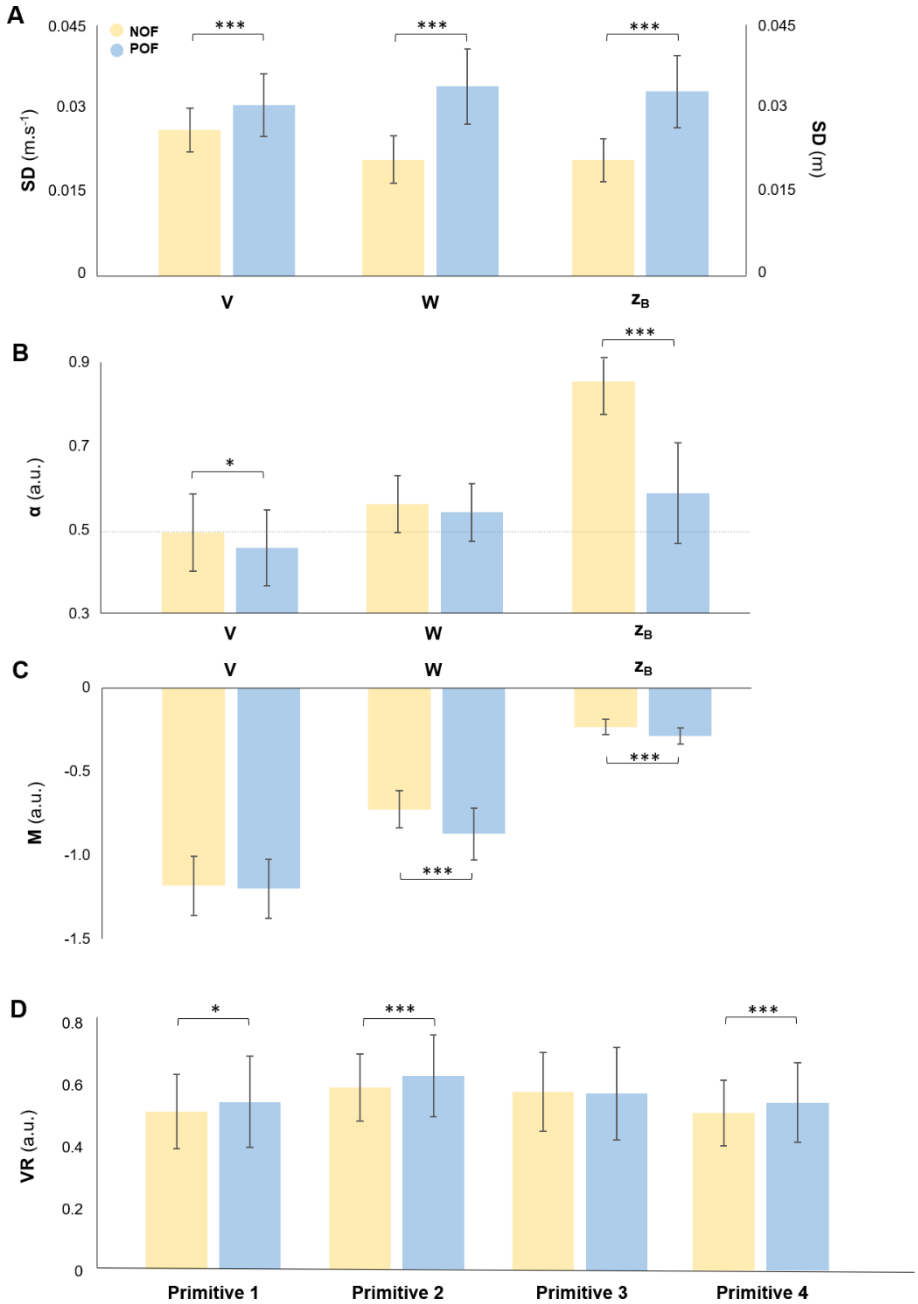

Figure 5. Main effect of *Optic flow* for **A)** standard deviation (SD), **B)** detrended fluctuation analysis (DFA) scaling exponent (α), **C)** least-squares regression linear slope (M) of step velocity (V), step width (W) and lateral body position (z_B), and **D)** variance ratio (VR) of each motor primitive. NOF: normal optic flow (yellow bars), POF: perturbed optic flow (blue bars). See legend of Figure 4 for details.

A significant main effect of *Walking condition* was found for α of W and α of V (respectively, Figures 6A and 6B). Post-hoc tests revealed a decrease in persistence of W in DTW-2b compared to STW conditions and a decrease in anti-persistence of V in DTW-3b compared to DTW-1b conditions.

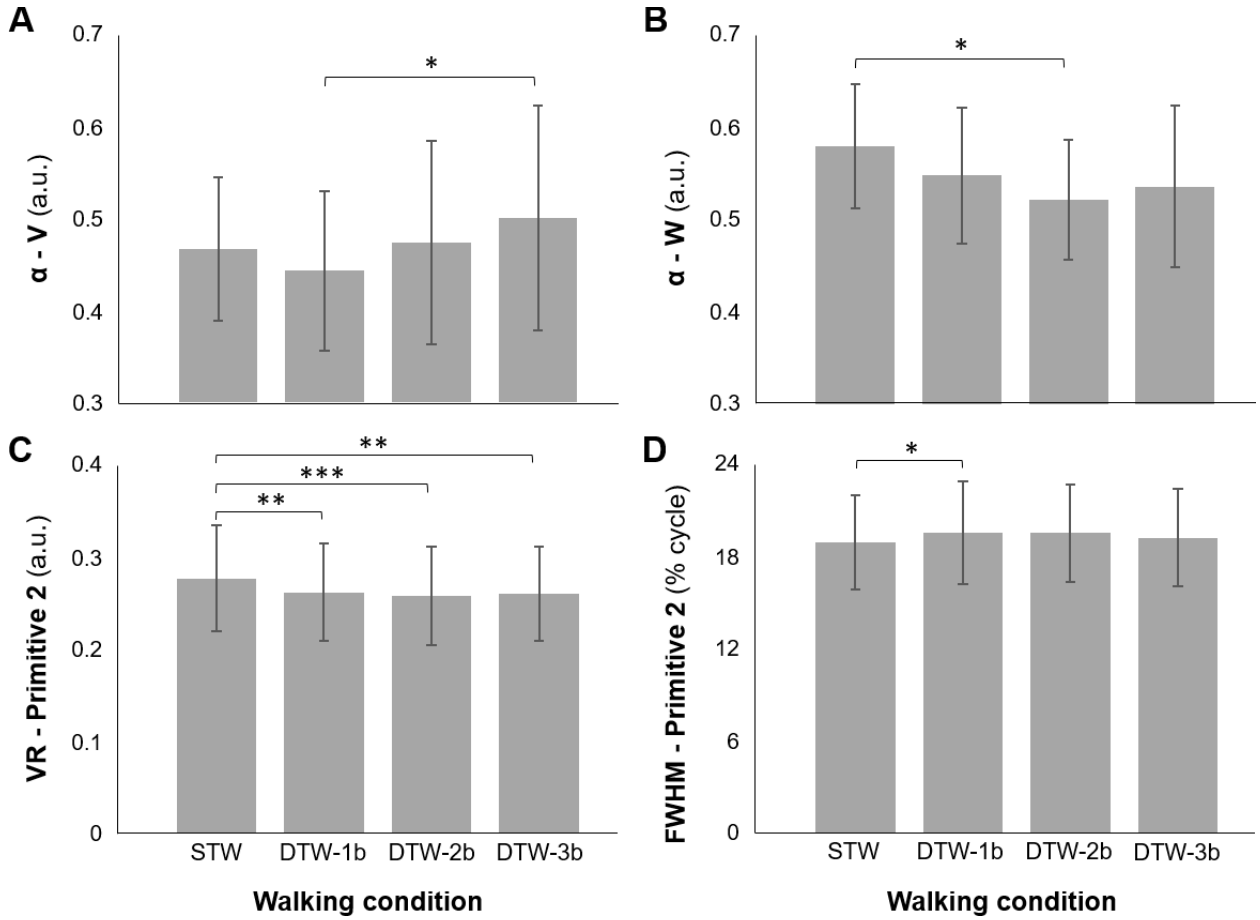

Figure 6. Main effect of *Walking condition* for detrended fluctuation analysis (DFA) scaling exponent (α) of **A)** step velocity (V) and **B)** step width (W), for **C)** variance ratio (VR, a.u.), and for **D)** full width at half maximum (FWHM, % cycle) of motor primitive 2. The four walking conditions: single-task walking (STW) and dual-task walking (DTW), *i.e.* walking while simultaneously responding to auditory 1-back (DTW-1b), 2-back (DTW-2b), and 3-back (DTW-3b) tasks are represented regardless of optical flow condition. *: significant differences between the four conditions (* $p < .05$, ** $p < .01$, *** $p < .001$).

Gait electromyography

Functional organization of muscle synergies

Analysis of the dimensionality of muscle synergies using NNMF revealed that 3 to 4 muscle synergies were sufficient to adequately capture the gait of young adults whatever the experimental condition considered (Figure 7). As the chi² test performed was non-significant (chi² = 1.81; theoretical critical threshold is set at 3.84), the variables were considered independent, and the *Optic Flow* had no significant impact on the number of synergies defined by VAF. Thus, although a model with three synergies was sufficient for several subjects, we chose to retain four synergies (VAF = 90.5 ± 2 %) because this was the

most frequent occurrence and it is consistent with the study by Clark et al. (60) which used the same experimental set-up (60).

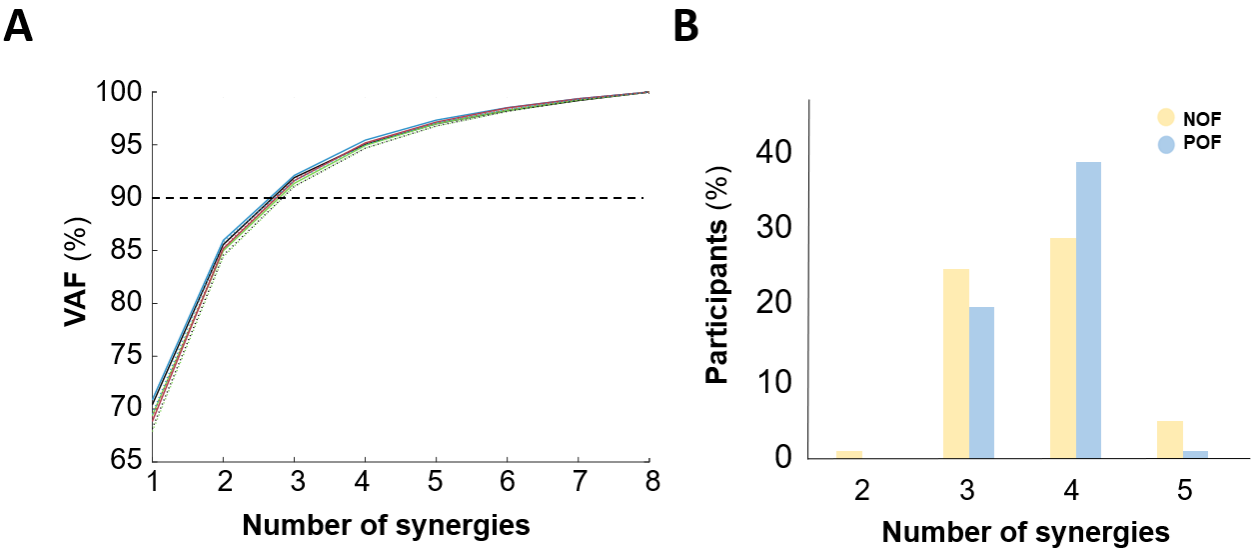

Figure 7. **A)** Mean variance accounted for (VAF) based on the number of synergies extracted by non-negative matrix factorization (NNMF) for all conditions combined: single-task walking (STW, black) and dual-task walking (DTW) 1-back (DTW-1b, green), 2-back (DTW-2b, blue) and 3-back (DTW-3b, red), performed under normal optic flow (NOF, solid lines) and perturbed optic flow (POF, dotted lines), and **B)** Percentage of participants (%) as a function of the number of synergies extracted by NNMF under normal optic flow (NOF, yellow bars) and perturbed optic flow (POF, blue bars).

Synergy 1 was active during damping and loading in early stance involving extensor muscles (*VM, RF* and *Gmed*). Synergy 2 was composed of the plantar flexors (*SOL* and *GM)* and was mainly active during propulsion and swing initiation. Synergy 3 mainly involves TA and, to a lesser extent, the quadriceps (*VM* and *RF*) during the initiation of each phase (stance and swing). Then, Synergy 4 includes activation of the hamstrings (*BF* and *ST*) in order to ensure the transition between the swing phase and the stance phase by decelerate the leg before the foot contacts the ground, and propel the body during early stance. The motor primitives and corresponding motor modules in normal and perturbed optic flow are shown in Figures 8A and 8B, respectively.

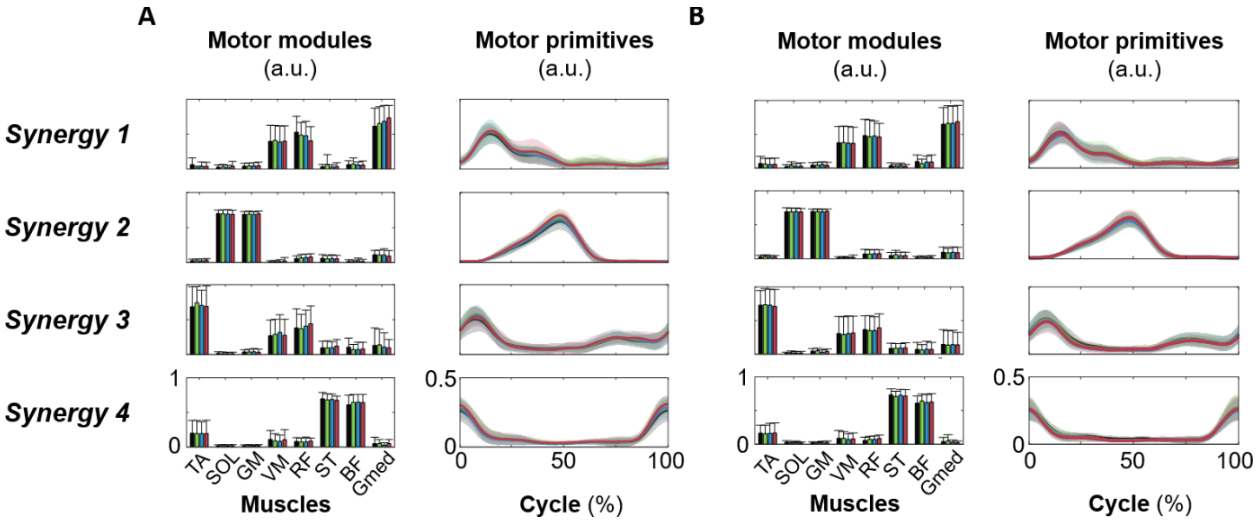

Figure 8. For each synergy, the motor module (spatial component) and motor primitive (temporal component) are displayed for the four walking conditions combined: single-task walking (STW, black) and dual-task walking (DTW) 1-back (DTW-1b, green), 2-back (DTW-2b, blue) and 3-back (DTW-3b, red), performed under **A)** normal optic flow (NOF) and **B)** perturbed optic flow (POF).

Motor module consistency

A positive correlation was observed for all motor modules on average, whatever the walking condition. The results suggested no impact of the WM load (similar modules) on motor module composition (Table 3).

Table 3. Motor module similarity (dot product, *r*) observed for each synergy between single-task walking (STW) and each dual-task walking (DTW) conditions, *i.e.* 1-back (DTW-1b), 2-back (DTW-2b) and 3-back (DTW-3b), under normal optic flow (NOF) and perturbed optic flow (POF), respectively. Mean, standard deviation, and percentage of participants for whom *r* > 0.8 are reported.

			NOF			POF	
Synergy	**Variables**	**DTW-1b**	**DTW-2b**	**DTW-3b**	**DTW-1b**	**DTW-2b**	**DTW-3b**
	Mean	0.92	0.88	0.86	0.88	0.92	0.98
1	SD	0.22	0.26	0.29	0.25	0.21	0.01
	% (r > 0.8)	93%	87%	87%	87%	93%	100%
	Mean	0.98	0.96	0.96	0.97	0.96	0.99
2	SD	0.06	0.09	0.09	0.07	0.08	0.01
	% (r > 0.8)	93%	93%	93%	93%	93%	100%
	Mean	0.95	0.92	0.89	0.95	0.92	0.96
3	SD	0.10	0.13	0.16	0.11	0.14	0.04
	% (r > 0.8)	93%	87%	80%	93%	80%	100%
	Mean	0.93	0.93	0.95	0.95	0.94	0.96
4	SD	0.13	0.09	0.06	0.06	0.11	0.06
	% (r > 0.8)	87%	93%	100%	100%	93%	93%

Motor primitive variability and duration

A significant main effect of *Optic flow* was found for VR values of motor primitives 1, 2 and 4 (Table 2, Figure S3). Post-hoc tests revealed increased VR values in POF compared to NOF conditions (Figure 5D). A significant main effect of *Walking condition* on VR values was found for the motor primitive 2. Post-hoc tests revealed decreased VR values in DTW-1b, DTW-2b and DTW-3b compared to STW conditions (Figure 6C). While there was no effect of *Optic flow* on FWHM values, a significant main effect of *Walking condition* was found for the motor primitive 2. Post-hoc tests revealed higher FWHM values in DTW-1b compared to STW conditions (Figure 6D).

DISCUSSION

The present study aimed to characterize cognitive involvement in gait control at the kinematic and neuromuscular levels in healthy young adults. The results confirmed the first hypothesis since kinematic (*i.e.* step parameters) and neuromuscular (*i.e.* motor primitives) variability was found to be greater under POF compared to NOF conditions, and young adults sought to counteract the disruption of optic flow by rapidly correcting task-relevant gait fluctuations. The second hypothesis was partially supported, since the depletion of cognitive resources through dual-tasking led to a reduction in kinematic and neuromuscular variability and looser regulation of task-relevant gait fluctuations, but this occurred to the same extent regardless of simultaneous WM load. Furthermore, the duration of the motor primitive of the synergy specific to propulsion during the stance phase was found to be increased, but only with the addition of a low-demand secondary task (1-back). Interestingly, in support of existing literature, the increase in WM load led to a prioritization of gait control in the ML direction over the AP direction. Lastly, the third hypothesis was partially supported, since the impact of POF on kinematic variability (step velocity) was reduced when a cognitive task was performed simultaneously, but this phenomenon was not more pronounced with increasing WM load, on the one hand, and was not found for other kinematic and neuromuscular variables, on the other. An explanation of this last, seemingly counter-intuitive result is proposed later in the discussion.

Regarding cognitive performance, as expected, cognitive performance decreased (greater TR and lower d'; 48, 69) and subjective mental workload increased (greater raw NASA-TLX score; 70) with increasing WM load, thus validating our incremental dual-task paradigm (3-back > 2-back > 1-back) under both single-task and dual-task conditions. In addition, participants reported a higher subjective mental workload under POF compared to both NOF and sitting (single-task) conditions. However,

similarly to Pechtl et al. (28), cognitive performance did not differ between the sitting and walking conditions, indicating that participants maintained their cognitive engagement and performance regardless of the context. Conversely, this finding contrasts with those from Kao and Pierro (40) who observed dual-task effects on cognitive performance under perturbed walking (*i.e.* continuous treadmill platform sways). The lack of interference of concurrent WM load on cognitive performance could be due to the perturbation modality, visual *vs* mechanical, which involves different mechanisms, and thus probably does not require the same demand in terms of attentional resources (26, 71). Hence, it is likely that the complexification of the locomotor task, through the use of visual perturbations, does not represent a sufficiently large threat to healthy young adults, in contrast to mechanical perturbations, so that they are able to maintain their engagement in the performance of a simultaneous cognitive task. Nevertheless, the fact that performance on the concurrent cognitive task was not altered facilitates interpretation of the adjustments made to gait control.

The effects of POF on gait control were observed at both the kinematic and neuromuscular levels. In line with previous studies, variability in mediolateral (z_B, W) and anteroposterior (V) kinematic parameters increased under POF (26, 72–75). This increased variability was also pointed out at the neuromuscular level with the increased variance ratio for three (1,2 and 4) of the four muscle synergies. To our knowledge, this is the first demonstration in the literature of a joint increase in variability at both the kinematic and neuromuscular levels following exposure of the locomotor system to a perturbation. On the other hand, contrary to what was expected, no change was observed either in the number of motor modules or in the duration (FWHM) of motor primitives under POF. Thus, in response to POF, the CNS maintains motor control by soliciting a limited number of robust motor synergies whose activation profiles are more variable. This low-level strategy is associated with a simultaneous increase in kinematic and neuromuscular variability.

To overcome the locomotor variability induced by visual perturbations, young adults exert greater cognitive control in order to preserve gait balance (*i.e.* global stability; 26). This strategy results in increased step width (*i.e.* a wider base of sustentation; 40, 76), tighter regulation (*i.e.* increased step-by-step corrections) of both lateral body position and step width, and reduced persistence of fluctuations in lateral body position (26, 27) under POF conditions. Furthermore, as in previous studies, corrections were tighter for step width than for lateral body position in all conditions (24, 26). Overall, these findings are consistent with multi-objective control simulations (24), according to which young adults increase the CNS control to enact greater corrections for deviations in both step

width and lateral body position in order to maintain a central position on the treadmill. Lastly, the antipersistence of step velocity fluctuations is increased in POF conditions ($\alpha < 0.5$), indicating tighter regulation of these fluctuations. These observations suggest overcorrection typical of less optimal regulation (22, 23, 77). Collectively, these results provide further evidence that cognitive involvement in locomotor control increases in the presence of a perturbation, here in the visual modality.

The interference effect of concurrent WM task on gait control was observed at both kinematic and neuromuscular levels. Precisely, at the neuromuscular level, an increase in the duration of the motor primitive 2 *(i.e.* plantar flexors) and a decrease in the variability of the same motor primitive were observed from the first level of WM load (*i.e.* DTM-1b, which mainly involves external focus of attention and relatively few central executive resources). These results suggest that participants rigidified their gait control when confronted with a simultaneous WM task, presumably to make treadmill walking more stable and safer, as previously suggested (15, 40, 79). This more rigid gait pattern under dual-task conditions proves effective, as evidenced by the absence of changes in gait steadiness (*i.e.* mean values of kinematic parameters). In sum, only plantar flexor activity during the propulsive phase was modulated by the CNS in response to increased WM load. These results highlight the flexibility of the CNS to modulate only one synergy, and not the others (*i.e.* synergies 1, 3 and 4), as previously observed in walk-run transition tasks (64, 78). Interestingly, the increase in the duration of the motor primitive 2 was only observed in DTW-1b, and not in DTW-2b and DTW-3b, the latter two inducing greater competition between the tasks at hand (*i.e.* locomotor and WM tasks) for limited attentional resources. These results corroborate those of Walsh (16), who observed no effect of a 7-in-7 backward counting task (*i.e.* a task that was also executive like the 2- and 3-back conditions) on FWHM values (note that, methodologically, FWHM values were calculated across all synergies, unlike in our study). A likely explanation is that, under the DTW-1b condition, parallel task processing is possible because the 1-back task requires no, or relatively few, central executive resources. Thus, the CNS was able to allocate some of these resources to motor control adjustments to increase global gait stability. Conversely, it is probable that most of the central executive resources were allocated to the execution of cognitive tasks under 2- and 3-back conditions (*i.e.* cognitive task prioritization in order to maintain performance), so that the remaining central executive resources were no longer sufficient to allow such motor control adjustments (80, 81).

This proposition is partially confirmed by the kinematic data. With the concomitant increase in WM load during walking, fluctuations in step width became more tightly regulated from the STW

condition to the DTW-2b condition. This tighter regulation was certainly enabled through the involvement of central executive processes (23, 77). Taken together, the decreased persistence of step width fluctuations and the increased duration of the motor primitive 2 involving the plantar flexors are consistent with the adoption of a more rigid gait pattern in the ML direction. Consequently, the search for greater global stability comes at the cost of lower flexibility. Conversely, fluctuations in step velocity became less tightly regulated from DTW-1b to DTW-3b; in other words, participants would no longer had sufficient central executive resources to correct fluctuations in step velocity in the AP direction as rapidly. This phenomenon was also found in a previous study, in which WM load was manipulated using a dichotic listening paradigm (23). Collectively, these findings provide further evidence that central executive processes are involved in the regulation of gait fluctuations relevant to the locomotor task goal (*i.e.* maintaining constant step velocity and lateral body position in the center of the treadmill) and that, with increasing WM load, participants prioritize gait control in the ML direction (*i.e.* tighter control) over the AP direction (*i.e.* looser control). In fact, it is likely that under higher WM load (*i.e.* DTW-3b), participants no longer had sufficient central executive resources, so that control of walking in the AP direction was neglected. Such a strategy allows for more efficient use of central executive resources, assuming that gait has passive dynamic stability in the AP direction and that active control is critically needed for balance maintenance in the ML direction (80, 81).

Lastly, an interaction effect was only observed for step velocity variability. This raises the question of why an interaction effect was found for this particular variable. A likely explanation is that the visual constraint (*i.e.* POF) applied in the ML direction increased step velocity variability by interfering with the mechanical constraint (*i.e.* treadmill moving at a constant speed) applied in the opposite, AP, direction. Young adults, by directing their attentional resources to the concurrent auditory task, may have paid less attention to visual information from the virtual environment, thus mitigating the impact of POF on gait control. Besides, from a methodological point of view, the use of a conservative statistical method (*i.e.* linear mixed-effects model with bootstrapping) may have limited interaction effects in our analyses compared to other studies (4, 26, 28).

A few methodological issues should be considered when interpreting the results of this study. First, STW conditions were systematically performed before DTW ones; indeed, STW conditions performed after the DTW ones were not included in the main analyses for the reasons mentioned in the *Supplementary material S1*. However, substantial initial familiarization to treadmill walking had

taken place beforehand in order to limit any possible learning effect. Second, treadmill walking was performed at a fixed speed (although self-selected by the participant). The differences between fixed-speed treadmill walking and overground walking (*i.e.* everyday walking) have been extensively studied and highlighted in many studies (82, 83). For example, some studies have observed a decrease in variability of several kinematic parameters during treadmill walking compared to overground walking (84, 85). This phenomenon has not prevented to observe the impact of visual and cognitive constraints on gait variability and, more broadly, on gait regulation. Furthermore, the use of fixed-speed treadmill walking was intended to explore the impact of experimental constraints on variables known to be regulated by the locomotor system, *i.e.* variables that allow the (implicit) goal of the locomotor task ("do not step off the AP and ML limits of the treadmill") to be satisfied.

In conclusion, this study replicated and extended previous research on how humans regulate gait from each step to the next to achieve goal-directed walking (Dingwell et al., 2010; Dingwell & Cusumano, 2015, 2019), through the use of a virtual reality-induced optic flow disruption paradigm to destabilize lateral gait balance and a dual-task paradigm to progressively deplete attentional resources that can be allocated to walking. These two paradigms have been used separately and together to gain a deeper understanding of how cognitive processes intervene in gait (stepping) regulation. This study has several strengths. To our knowledge, it is the first study to characterize cognitive contributions to walking by focusing on potentially relevant gait variables, assessing different aspects (dimensions) of these variables (steadiness, variability, complexity), and linking kinematic to neuromuscular responses. The results revealed that humans optimally regulate their gait to effectively cope with interacting task and environmental constraints, by maintaining relatively stable muscle synergies, flexibly allocating attentional resources to the two tasks at hand, and prioritizing gait variables most relevant to the specific goal-directed locomotor tasks. Specifically, an increase in WM load during walking led first to an increase in the motor primitive duration of propulsion-specific synergy, followed by stiffer control in the ML direction and looser control in the AP direction. Future research is encouraged by these results to examine compensatory strategies employed by patients with peripheral or central deficits or the elderly to counteract the negative effects of aging or underlying pathological processes on the regulation of gait control in environments that are unstable.

DATA AVAILABILITY

All data collected are available and can be downloaded from Dryad platform (http://doi.org/10.5061/dryad.bnzs7h4ds).

ACKNOWLEDGMENTS

We are very grateful to the participants who took part in the study, and to the Interdisciplinary Center for Virtual Reality (CIREVE) in Caen for their unwavering help and support.

GRANTS

This work was funded by the National Agency for Research and Technology (ANRT) through a CIFRE doctoral fellowship awarded to Valentin Lana and the partnership between the NOVATEX MEDICAL company and the COMETE and GIPSA-Lab laboratories (CIFRE N°2018/0478).

DISCLOSURES

No conflicts of interest, financial or otherwise, are declared by the authors.

AUTHOR CONTRIBUTIONS

L.M.D., J.F., V.L. designed the whole study; N.L. conceived the virtual environment; L.M.D., J.F., V.L. conceived the data analysis plan; V.C., V.L., T.R. collected the data; V.C., V.L. analyzed the data; L.M.D., J.F., V.L. interpreted the results; L.M.D., J.F., V.L. wrote the manuscript. L.M.D., J.F., V.L., E.V. obtained funding. All authors read and approved the final version of the manuscript before submission.

REFERENCES

1. **Brown TG**. The Intrinsic Factors in the Act of Progression in the Mammal. *Proceedings of the Royal Society of London Series B, Containing Papers of a Biological Character* 84: 308–319, 1911.

2. **Takakusaki K**. Functional Neuroanatomy for Posture and Gait Control. *JMD* 10: 1–17, 2017. doi: 10.14802/jmd.16062.

3. **Kuhman D**, **Hurt CP**, **Reed WR**, **Rosenblatt NJ**, **Visscher K**, **Walker H**. Gait Adaptability with Healthy Aging and Parkinson's Disease. .

4. **Malcolm BR**, **Foxe JJ**, **Butler JS**, **Molholm S**, **De Sanctis P**. Cognitive load reduces the effects of optic flow on gait and electrocortical dynamics during treadmill walking. *Journal of Neurophysiology* 120: 2246–2259, 2018. doi: 10.1152/jn.00079.2018.

5. **Takakusaki K**. Neurophysiology of gait: From the spinal cord to the frontal lobe: Neurophysiology of Gait. *Mov Disord* 28: 1483–1491, 2013. doi: 10.1002/mds.25669.

6. **Kiehn O**. Decoding the organization of spinal circuits that control locomotion. *Nat Rev Neurosci* 17: 224–238, 2016. doi: 10.1038/nrn.2016.9.

7. **Grillner S**, **Wallén P**, **Saitoh K**, **Kozlov A**, **Robertson B**. Neural bases of goal-directed locomotion in vertebrates—An overview. *Brain Research Reviews* 57: 2–12, 2008. doi: 10.1016/j.brainresrev.2007.06.027.

8. **Hamacher D**, **Herold F**, **Wiegel P**, **Hamacher D**, **Schega L**. Brain activity during walking: A systematic review. *Neurosci Biobehav Rev* 57: 310–327, 2015. doi: 10.1016/j.neubiorev.2015.08.002.

9. **Bernstein NA**. The co-ordination and regulation of movements [Online]. Pergamon Press. http://books.google.com/books?id=F9dqAAAAMAAJ [13 Feb. 2022].

10. **d'Avella A**, **Saltiel P**, **Bizzi E**. Combinations of muscle synergies in the construction of a natural motor behavior. *Nat Neurosci* 6: 300–308, 2003. doi: 10.1038/nn1010.

11. **Bizzi E**, **Cheung VCK**. The neural origin of muscle synergies. *Front Comput Neurosci* 7, 2013. doi: 10.3389/fncom.2013.00051.

12. **Ting LH**, **Chiel HJ**, **Trumbower RD**, **Allen JL**, **McKay JL**, **Hackney ME**, **Kesar TM**. Neuromechanical Principles Underlying Movement Modularity and Their Implications for Rehabilitation. *Neuron* 86: 38–54, 2015. doi: 10.1016/j.neuron.2015.02.042.

13. **Allen JL**, **Franz JR**. The motor repertoire of older adult fallers may constrain their response to balance perturbations. *Journal of Neurophysiology* 120: 2368–2378, 2018. doi: 10.1152/jn.00302.2018.

14. **Santuz A**, **Brüll L**, **Ekizos A**, **Schroll A**, **Eckardt N**, **Kibele A**, **Schwenk M**, **Arampatzis A**. Neuromotor Dynamics of Human Locomotion in Challenging Settings. *iScience* 23: 100796, 2020. doi: 10.1016/j.isci.2019.100796.

15. **Martino G**, **Ivanenko YP**, **d'Avella A**, **Serrao M**, **Ranavolo A**, **Draicchio F**, **Cappellini G**, **Casali C**, **Lacquaniti F**. Neuromuscular adjustments of gait associated with unstable conditions. *Journal of Neurophysiology* 114: 2867–2882, 2015. doi: 10.1152/jn.00029.2015.

16. **Walsh GS**. Dynamics of Modular Neuromotor Control of Walking and Running during Single and Dual Task Conditions. *Neuroscience* 465: 1–10, 2021. doi: 10.1016/j.neuroscience.2021.04.004.

17. **Al-Yahya E**, **Dawes H**, **Smith L**, **Dennis A**, **Howells K**, **Cockburn J**. Cognitive motor interference while walking: A systematic review and meta-analysis. *Neuroscience & Biobehavioral Reviews* 35: 715–728, 2011. doi: 10.1016/j.neubiorev.2010.08.008.

18. **Sheridan PL**, **Solomont J**, **Kowall N**, **Hausdorff JM**. Influence of Executive Function on Locomotor Function: Divided Attention Increases Gait Variability in Alzheimer's Disease. *Journal of the American Geriatrics Society* 51: 1633–1637, 2003. doi: 10.1046/j.1532-5415.2003.51516.x.

19. **Holtzer R**, **Verghese J**, **Xue X**, **Lipton RB**. Cognitive processes related to gait velocity: results from the Einstein Aging Study. *Neuropsychology* 20: 215–223, 2006. doi: 10.1037/0894-4105.20.2.215.

20. **Alvarez JA**, **Emory E**. Executive Function and the Frontal Lobes: A Meta-Analytic Review. *Neuropsychol Rev* 16: 17–42, 2006. doi: 10.1007/s11065-006-9002-x.

21. **Schättin A**, **Arner R**, **Gennaro F**, **de Bruin ED**. Adaptations of Prefrontal Brain Activity, Executive Functions, and Gait in Healthy Elderly Following Exergame and Balance Training: A Randomized-Controlled Study. *Front Aging Neurosci* 8: 278, 2016. doi: 10.3389/fnagi.2016.00278.

22. **Dingwell JB**, **John J**, **Cusumano JP**. Do Humans Optimally Exploit Redundancy to Control Step Variability in Walking? *PLoS Comput Biol* 6: e1000856, 2010. doi: 10.1371/journal.pcbi.1000856.

23. **Decker LM**, **Cignetti F**, **Stergiou N**. Executive function orchestrates regulation of task-relevant gait fluctuations. *Gait & Posture* 38: 537–540, 2013. doi: 10.1016/j.gaitpost.2012.12.018.

24. **Dingwell JB**, **Cusumano JP**. Humans use multi-objective control to regulate lateral foot placement when walking. *PLoS Comput Biol* 15: e1006850, 2019. doi: 10.1371/journal.pcbi.1006850.

25. **Kazanski ME**, **Cusumano JP**, **Dingwell JB**. Rethinking margin of stability: Incorporating step-to-step regulation to resolve the paradox. *Journal of Biomechanics* 144: 111334, 2022. doi: 10.1016/j.jbiomech.2022.111334.

26. **Kazanski ME**, **Cusumano JP**, **Dingwell JB**. How healthy older adults regulate lateral foot placement while walking in laterally destabilizing environments. *Journal of Biomechanics* 104: 109714, 2020. doi: 10.1016/j.jbiomech.2020.109714.

27. **Render AC**, **Kazanski ME**, **Cusumano JP**, **Dingwell JB**. Walking humans trade off different task goals to regulate lateral stepping. *Journal of Biomechanics* 119: 110314, 2021. doi: 10.1016/j.jbiomech.2021.110314.

28. **Pechtl KS**, **Jennings JR**, **Redfern MS**. Optic flow and attention alter locomotion differently in the young and old. *Gait & Posture* 76: 1–6, 2020. doi: 10.1016/j.gaitpost.2019.10.022.

29. **Blomberg R**, **Johansson Capusan A**, **Signoret C**, **Danielsson H**, **Rönnberg J**. The Effects of Working Memory Load on Auditory Distraction in Adults With Attention Deficit Hyperactivity Disorder. *Front Hum Neurosci* 15: 771711, 2021. doi: 10.3389/fnhum.2021.771711.

30. **McAndrew PM**, **Wilken JM**, **Dingwell JB**. Dynamic stability of human walking in visually and mechanically destabilizing environments. *Journal of Biomechanics* 44: 644–649, 2011. doi: 10.1016/j.jbiomech.2010.11.007.

31. **Vuillemin A**, **Oppert J-M**, **Guillemin F**, **Essermeant L**, **Fontvieille A-M**, **Galan P**, **Kriska AM**, **Hercberg S**. Self-administered questionnaire compared with interview to assess past-year physical activity: *Medicine & Science in Sports & Exercise* 32: 1119–1124, 2000. doi: 10.1097/00005768-200006000-00013.

32. **van Melick N**, **Meddeler BM**, **Hoogeboom TJ**, **Nijhuis-van der Sanden MWG**, **van Cingel REH**. How to determine leg dominance: The agreement between self-reported and observed performance in healthy adults. *PLoS ONE* 12: e0189876, 2017. doi: 10.1371/journal.pone.0189876.

33. **Jordan K**, **Challis JH**, **Newell KM**. Walking speed influences on gait cycle variability. *Gait & Posture* 26: 128–134, 2007. doi: 10.1016/j.gaitpost.2006.08.010.

34. **Schaefer S**, **Jagenow D**, **Verrel J**, **Lindenberger U**. The influence of cognitive load and walking speed on gait regularity in children and young adults. *Gait & Posture* 41: 258–262, 2015. doi: 10.1016/j.gaitpost.2014.10.013.

35. **Hart SG**, **Staveland LE**. Development of NASA-TLX (Task Load Index): Results of Empirical and Theoretical Research. In: *Advances in Psychology*. Elsevier, p. 139–183.

36. **Cegarra J**, **Morgado N**. Étude des propriétés de la version francophone du NASA-TLX. .

37. **Bardy BG**, **Warren WH**, **Kay BA**. Motion parallax is used to control postural sway during walking. *Exp Brain Res* 111: 271–282, 1996. doi: 10.1007/BF00227304.

38. **Salinas MM**, **Wilken JM**, **Dingwell JB**. How humans use visual optic flow to regulate stepping during walking. *Gait & Posture* 57: 15–20, 2017. doi: 10.1016/j.gaitpost.2017.05.002.

39. **Grissmann S**, **Faller J**, **Scharinger C**, **Spüler M**, **Gerjets P**. Electroencephalography Based Analysis of Working Memory Load and Affective Valence in an N-back Task with Emotional Stimuli. *Front Hum Neurosci* 11: 616, 2017. doi: 10.3389/fnhum.2017.00616.

40. **Kao P-C**, **Pierro MA**. Motor adaptation to cognitive challenges and walking perturbations in healthy young adults. *Gait & Posture* 92: 167–175, 2022. doi: 10.1016/j.gaitpost.2021.11.030.

41. **Owen AM**, **McMillan KM**, **Laird AR**, **Bullmore E**. N-back working memory paradigm: A meta-analysis of normative functional neuroimaging studies. *Hum Brain Mapp* 25: 46–59, 2005. doi: 10.1002/hbm.20131.

42. **Szmalec A**, **Verbruggen F**, **Vandierendonck A**, **Kemps E**. Control of interference during working memory updating. *Journal of Experimental Psychology: Human Perception and Performance* 37: 137–151, 2011. doi: 10.1037/a0020365.

43. **Vaughan CL**, **Davis BL**, **O'Connor JC**. Dynamics of Human Gait [Online]. https://archive.org/details/dynamicsofhumang0000unse [15 Feb. 2022].

44. **Davis RB**, **Õunpuu S**, **Tyburski D**, **Gage JR**. A gait analysis data collection and reduction technique. *Human Movement Science* 10: 575–587, 1991. doi: 10.1016/0167-9457(91)90046-Z.

45. **De Luca CJ**. The Use of Surface Electromyography in Biomechanics. *Journal of Applied Biomechanics* 13: 135–163, 1997. doi: 10.1123/jab.13.2.135.

46. **Hermens HJ**, **Freriks B**, **Disselhorst-Klug C**, **Rau G**. Development of recommendations for SEMG sensors and sensor placement procedures. *Journal of Electromyography and Kinesiology* 10: 361–374, 2000. doi: 10.1016/S1050-6411(00)00027-4.

47. **Hart SG**. Nasa-Task Load Index (NASA-TLX); 20 Years Later. *Proceedings of the Human Factors and Ergonomics Society Annual Meeting* 50: 904–908, 2006. doi: 10.1177/154193120605000909.

48. **Pelegrina S**, **Lechuga MT**, **García-Madruga JA**, **Elosúa MR**, **Macizo P**, **Carreiras M**, **Fuentes LJ**, **Bajo MT**. Normative data on the n-back task for children and young adolescents. *Front Psychol* 6, 2015. doi: 10.3389/fpsyg.2015.01544.

49. **Kumar V**, **Nichenmetla S**, **Chhabra H**, **Sreeraj VS**, **Rao NP**, **Kesavan M**, **Varambally S**, **Venkatasubramanian G**, **Gangadhar BN**. Prefrontal cortex activation during working memory task in schizophrenia: A fNIRS study. *Asian Journal of Psychiatry* 56: 102507, 2021. doi: 10.1016/j.ajp.2020.102507.

50. **Michail G**, **Senkowski D**, **Niedeggen M**, **Keil J**. Memory Load Alters Perception-Related Neural Oscillations during Multisensory Integration. *J Neurosci* 41: 1505–1515, 2021. doi: 10.1523/JNEUROSCI.1397-20.2020.

51. **Haatveit BC**, **Sundet K**, **Hugdahl K**, **Ueland T**, **Melle I**, **Andreassen OA**. The validity of *d* prime as a working memory index: Results from the "Bergen *n* -back task." *Journal of Clinical and Experimental Neuropsychology* 32: 871–880, 2010. doi: 10.1080/13803391003596421.

52. **Zeni JA**, **Richards JG**, **Higginson JS**. Two simple methods for determining gait events during treadmill and overground walking using kinematic data. *Gait & Posture* 27: 710–714, 2008. doi: 10.1016/j.gaitpost.2007.07.007.

53. **Peng C-K**, **Mietus J**, **Hausdorff JM**, **Havlin S**, **Stanley HE**, **Goldberger AL**. Long-range anticorrelations and non-Gaussian behavior of the heartbeat. *Phys Rev Lett* 70: 1343–1346, 1993. doi: 10.1103/PhysRevLett.70.1343.

54. **Hausdorff JM**, **Mitchell SL**, **Firtion R**, **Peng CK**, **Cudkowicz ME**, **Wei JY**, **Goldberger AL**. Altered fractal dynamics of gait: reduced stride-interval correlations with aging and Huntington's disease. *Journal of Applied Physiology* 82: 262–269, 1997. doi: 10.1152/jappl.1997.82.1.262.

55. **Damouras S**, **Chang MD**, **Sejdić E**, **Chau T**. An empirical examination of detrended fluctuation analysis for gait data. *Gait & Posture* 31: 336–340, 2010. doi: 10.1016/j.gaitpost.2009.12.002.

56. **Phinyomark A**, **Larracy R**, **Scheme E**. Fractal Analysis of Human Gait Variability via Stride Interval Time Series. *Front Physiol* 11: 333, 2020. doi: 10.3389/fphys.2020.00333.

57. **Dingwell JB**, **Cusumano JP**. Identifying Stride-To-Stride Control Strategies in Human Treadmill Walking. *PLoS ONE* 10: e0124879, 2015. doi: 10.1371/journal.pone.0124879.

58. **Garofolini A**, **Mickle KJ**, **McLaughlin P**, **Taylor SB**. Insight into the hierarchical control governing leg stiffness during the stance phase of running. *Sci Rep* 12: 12123, 2022. doi: 10.1038/s41598-022-16263-7.

59. **Lee DD**, **Seung HS**. Algorithms for Non-negative Matrix Factorization. .

60. **Clark DJ**, **Ting LH**, **Zajac FE**, **Neptune RR**, **Kautz SA**. Merging of Healthy Motor Modules Predicts Reduced Locomotor Performance and Muscle Coordination Complexity Post-Stroke. *Journal of Neurophysiology* 103: 844–857, 2010. doi: 10.1152/jn.00825.2009.

61. **Torres-Oviedo G**, **Macpherson JM**, **Ting LH**. Muscle Synergy Organization Is Robust Across a Variety of Postural Perturbations. *Journal of Neurophysiology* 96: 1530–1546, 2006. doi: 10.1152/jn.00810.2005.

62. **Hershler C**, **Milner M**. An Optimality Criterion for Processing Electromyographic (EMG) Signals Relating to Human Locomotion. *IEEE Transactions on Biomedical Engineering* BME-25: 413–420, 1978. doi: 10.1109/TBME.1978.326338.

63. **Kadaba MP**, **Wootten ME**, **Gainey J**, **Cochran GVB**. Repeatability of phasic muscle activity: Performance of surface and intramuscular wire electrodes in gait analysis. *Journal of Orthopaedic Research* 3: 350–359, 1985. doi: 10.1002/jor.1100030312.

64. **Cappellini G**, **Ivanenko YP**, **Poppele RE**, **Lacquaniti F**. Motor Patterns in Human Walking and Running. *Journal of Neurophysiology* 95: 3426–3437, 2006. doi: 10.1152/jn.00081.2006.

65. **Bates D**, **Mächler M**, **Bolker B**, **Walker S**. Fitting Linear Mixed-Effects Models Using **lme4**. *J Stat Soft* 67, 2015. doi: 10.18637/jss.v067.i01.

66. **Kuznetsova A**, **Brockhoff PB**, **Christensen RHB**. **lmerTest** Package: Tests in Linear Mixed Effects Models. *J Stat Soft* 82, 2017. doi: 10.18637/jss.v082.i13.

67. **Halekoh U**, **Højsgaard S**. A Kenward-Roger Approximation and Parametric Bootstrap Methods for Tests in Linear Mixed Models - The *R* Package **pbkrtest**. *J Stat Soft* 59, 2014. doi: 10.18637/jss.v059.i09.

68. **R Core Team**. R: A language and environment for statistical computing. [Online]. R Foundation for Statistical Computing,: 2022. https://www.R-project.org/.

69. **Lamichhane B**, **Westbrook A**, **Cole MW**, **Braver TS**. Exploring brain-behavior relationships in the N-back task. *NeuroImage* 212: 116683, 2020. doi: 10.1016/j.neuroimage.2020.116683.

70. **Sadeghian M**, **Yazdanirad S**, **Mousavi SM**, **Jafari MJ**, **Khavanin A**, **Khodakarim S**, **Jafarpishe AS**. Effect of tonal noise and task difficulty on electroencephalography and cognitive performance. .

71. **Rafiee S**, **Kiemel T**. Multiple strategies to correct errors in foot placement and control speed in human walking. *Exp Brain Res* 238: 2947–2963, 2020. doi: 10.1007/s00221-020-05949-x.

72. **Osaba MY**, **Martelli D**, **Prado A**, **Agrawal SK**, **Lalwani AK**. Age-related differences in gait adaptations during overground walking with and without visual perturbations using a virtual reality headset. *Sci Rep* 10: 15376, 2020. doi: 10.1038/s41598-020-72408-6.

73. **Selgrade BP**, **Meyer D**, **Sosnoff JJ**, **Franz JR**. Can optical flow perturbations detect walking balance impairment in people with multiple sclerosis? *PLoS ONE* 15: e0230202, 2020. doi: 10.1371/journal.pone.0230202.

74. **Dingwell JB**, **Cusumano JP**, **Rylander JH**, **Wilken JM**. How persons with transtibial amputation regulate lateral stepping while walking in laterally destabilizing environments. *Gait & Posture* 83: 88–95, 2021. doi: 10.1016/j.gaitpost.2020.09.031.

75. **Song K**, **Franz JR**, **Wikstrom EA**. Optical flow balance perturbations alter gait kinematics and variability in chronic ankle instability patients. *Gait & Posture* 92: 271–276, 2022. doi: 10.1016/j.gaitpost.2021.12.001.

76. **Beurskens R**, **Wilken JM**, **Dingwell JB**. Dynamic stability of individuals with transtibial amputation walking in destabilizing environments. *Journal of Biomechanics* 47: 1675–1681, 2014. doi: 10.1016/j.jbiomech.2014.02.033.

77. **Decker LM**, **Cignetti F**, **Potter JF**, **Studenski SA**, **Stergiou N**. Use of Motor Abundance in Young and Older Adults during Dual-Task Treadmill Walking. *PLoS ONE* 7: e41306, 2012. doi: 10.1371/journal.pone.0041306.

78. **Hagio S**, **Fukuda M**, **Kouzaki M**. Identification of muscle synergies associated with gait transition in humans. *Front Hum Neurosci* 9, 2015. doi: 10.3389/fnhum.2015.00048.

79. **Verrel J**, **Lövdén M**, **Schellenbach M**, **Schaefer S**, **Lindenberger U**. Interacting effects of cognitive load and adult age on the regularity of whole-body motion during treadmill walking. *Psychology and Aging* 24: 75–81, 2009. doi: 10.1037/a0014272.

80. **Bauby CE**, **Kuo AD**. Active control of lateral balance in human walking. *Journal of Biomechanics* 33: 1433–1440, 2000. doi: 10.1016/S0021-9290(00)00101-9.

81. **O'Connor SM**, **Kuo AD**. Direction-Dependent Control of Balance During Walking and Standing. *Journal of Neurophysiology* 102: 1411–1419, 2009. doi: 10.1152/jn.00131.2009.

82. **Dingwell JB**, **Cusumano JP**, **Cavanagh PR**, **Sternad D**. Local Dynamic Stability Versus Kinematic Variability of Continuous Overground and Treadmill Walking. *Journal of Biomechanical Engineering* 123: 27–32, 2001. doi: 10.1115/1.1336798.

83. **Wrightson JG**, **Schäfer L**, **Smeeton NJ**. Dual-task prioritization during overground and treadmill walking in healthy adults. *Gait & Posture* 75: 109–114, 2020. doi: 10.1016/j.gaitpost.2019.08.007.

84. **Hollman JH**, **Watkins MK**, **Imhoff AC**, **Braun CE**, **Akervik KA**, **Ness DK**. A comparison of variability in spatiotemporal gait parameters between treadmill and overground walking conditions. *Gait & Posture* 43: 204–209, 2016. doi: 10.1016/j.gaitpost.2015.09.024.

85. **Wrightson JG**, **Smeeton NJ**. Walking modality, but not task difficulty, influences the control of dual-task walking. *Gait & Posture* 58: 136–138, 2017. doi: 10.1016/j.gaitpost.2017.07.042.